Dopant Orientation Dynamics in Doped Second-Order Nonlinear Optical Amorphous Polymers. 1. Effects of Temperature above and below T_g in Corona-Poled Films

Hilary L. Hampsch,[1a] Jian Yang,[1b] George K. Wong,[1b] and John M. Torkelson*,[1a,c]

Department of Materials Science and Engineering, Department of Physics and Astronomy, and Department of Chemical Engineering, Northwestern University, Evanston, Illinois 60208

Received October 24, 1989; Revised Manuscript Received February 16, 1990

ABSTRACT: The dynamics of the rotation of dopants dispersed in amorphous polymers have been studied using second harmonic generation (SHG), a nonlinear optical technique measuring frequency doubling. Corona poling is used to orient the dopants into the noncentrosymmetric structure required to obtain the SHG signal. The SHG intensity is sensitive to the dopant rotation, which is a function of the surrounding local polymer microenvironment, including segmental mobility and local free volume and the electric field across the film. The second harmonic coefficient, d_{film}, is related to the angle between the applied poling field and dopant axis parallel to the molecular dipole moment and to $[I_{film}]^{1/2}$, where I_{film} is the SHG intensity of the poled film. The effect of temperature above and below the glass transition on dopant rotation and polymer relaxations has been examined. As temperature increases, the rate of dopant orientation during poling increases. When the applied field is removed, the large SHG intensity drop reported for in situ contact-poled, doped films is not seen in these corona-poled, doped systems. The temporal stability of the SHG intensity following removal of the applied corona decreases with increasing temperature but does not decay in a manner described by a single or stretched exponential equation. Both the maintenance of the dopant orientation and the complicated SHG intensity decay relate to the persistence of the corona-induced field across the polymer film, due at least in part to a time-dependent retention of surface charge on the dielectric. The induced surface charge and the polymer relaxation behavior and their effects on the observed temporal stability of the SHG intensity as a function of temperature must be considered. Surface voltage decay following poling has been measured with an electrostatic voltmeter, and the magnitude and time scale of the surface charge persistence have been determined. A very small amount of charge remains on the film surface following poling but is still of sufficient magnitude to affect significantly dopant orientation in the glassy matrix.

Introduction

Glassy polymer behavior at temperatures well below the glass transition has been difficult to study at the molecular level. Recent studies involving second-order nonlinear optical (NLO) techniques have been shown to be sensitive in probing relaxation phenomena in glassy polymers at room temerature[2-5] at the molecular level. Optical techniques such as second harmonic generation (SHG), conversion of light of frequency ω to light of frequency 2ω, can be performed as a function of time to examine the temporal stability of oriented NLO dopants dispersed in a glassy polymer. The dopants must be oriented noncentrosymmetrically in the polymer matrix for SHG to occur. Information can be obtained about relaxation and mobility phenomena and local free volume microenvironments by examining dopant orientation in the polymer matrix as a function of temperature. It is also important to note that knowledge of the temporal and thermal stability of the SHG intensity is required for device applications of these polymeric NLO materials such as spatial light modulators, waveguides, and optical switches.[6] The importance of understanding the basic polymer physics of these materials for device applications has only recently been emphasized in the literature.[3-4,7,8]

The SHG technique is sensitive to dopant rotational mobility. The initial local free volume surrounding the dopant and changes with time in the local microenvironment thus lead to changes in the SHG intensity.[3,4] Electric field induced dopant orientation occurs in regions of sufficient local free volume and mobility. The dopant disorientation is due to mobility of the polymer chains and local free volume present in the vicinity of the dopant; the relaxations of the polymer and the presence of local free volume prevent the "freezing in" of the imposed orientation.

Other optical techniques[9,10] have been used to examine dopant orientation or rotation in glassy polymers. Fluorescence anisotropy[9] can be used to study glassy behavior on a molecular level but is limited in studying temporal changes in the material due to the length of time required to obtain each data set. In contrast, the SHG experiment can be used to measure dopant orientation and NLO properties continuously over a wide variety of time scales and a range of temperatures from well below to well above the glass transition temperature, T_g. Fourier transform infrared dichroism experiments[10] require a high degree of orientation to achieve sufficient sensitivity but are able to relate measurements to surface orientation or polymer chain relaxations for systems near or above T_g. High SHG signal intensities are observed both above and below T_g as long as there is enough mobility in the matrix for at least a small fraction of the NLO dopants to rotate in response to an imposed electric field. Small changes in dopant rotation can readily be detected as a function of time without causing irreversible change to the matrix or dopant as may occur in a photoisomerization[11,12] or mechanical[13] experiment. The sensitivity of this optical technique for measuring glassy behavior as a function of temperature is greater than index of refraction experiments.[14] As will be shown, dopant rotation in polymers with T_g's on the order of 100 °C can be examined at room temperature[3c,5] over reasonable time scales, as well as at higher temperatures. These experiments examine

* To whom correspondence should be addressed.

0024-9297/90/2223-3640$02.50/0

the effect of temperature on the temporal stability of NLO dopant orientation in corona-poled, doped poly(methyl methacrylate) (PMMA) and polystyrene (PS) matrices. The effect of polymer relaxations and the corona discharge induced electric field on the observed SHG intensity is considered.

Second Harmonic Generation

SHG is a special case of frequency mixing occurring when light waves of frequency ω passing through an array of molecules interact with them in such a way as to produce coherent light waves at 2ω.[15] NLO effects occur at the molecular level in the dopants due to a deviation from a harmonic electronic potential energy.[6] Typical dopants have a conjugated π-electron system with an electron donor and electron acceptor on either end, creating a large molecular hyperpolarizability β along the transition dipole axis.[6,15] Second-order NLO properties, including SHG, are described by the second-order susceptibility $\chi^{(2)}(-2\omega;\omega,\omega)$ tensor in the relationship for the bulk material polarization, $\mathbf{P}$[15]

$$\mathbf{P} = \chi^{(1)}\cdot\mathbf{E}(\omega) + \chi^{(2)}\cdot\mathbf{E}(\omega)\mathbf{E}(\omega) + \chi^{(3)}\cdot\mathbf{E}(\omega)\mathbf{E}(\omega)\mathbf{E}(\omega) + \ldots \quad (1)$$

The susceptibility tensors $\chi^{(n)}$ measure the macroscopic compliance of the electrons.[6] Since the second-order polarization is proportional to the optical field squared, SHG is zero in a centrosymmetric system. Thus to induce SHG, NLO dopants must be oriented noncentrosymmetrically in the polymer matrix.[3-8,15,16]

When the poled, doped films are modeled with a free-gas approximation, the second-order susceptibilities are given by[6,15]

$$\chi^{(2)}_{333} = NF\beta_{zzz}\langle\cos^3\theta\rangle \quad (2)$$

where N is the number of chromophores and F is a dimensionless field factor of order one. The subscript "3" refers to the direction of the poling field, and "z" represents the axis of the molecule parallel to the molecular dipole moment (assuming $\beta = \beta_{zzz}$).[6,15] θ represents the angle between the z and 3 directions. The second harmonic coefficient tensor, $\mathbf{d}$, defined[15] as $\mathbf{d}(-2\omega;\omega,\omega) = (1/2)\chi^{(2)}(-2\omega;\omega,\omega)$, is conventionally used for experimental results as opposed to $\chi^{(2)}$, which is used in theoretical calculations. Relationships between experimentally measured parameters and relative values for $\chi^{(2)}_{333}(-2\omega;\omega,\omega)$ or $d_{333}(-2\omega;\omega,\omega)$ (hereafter referred to as d_{333} or d) have been developed.[6,7,15c] For the experiments described here the approximate relationship for the measured intensities, an effective second harmonic coefficient d_{film} ($\neq d_{333}$ as the sample is not perpendicular to the beam), and the optical parameters can be shown to be[5,6a,15c]

$$d_{film} \sim (I_{film}/I_Q)^{1/2}(2/\pi)(n^3/l^2)_{film}^{1/2}(l_c^2/n^3)_Q^{1/2}d_Q \quad (3)$$

where Q represents the quartz reference, I is the SHG intensity, I_{film}/I_Q is the experimentaly measured intensity ratio, n is the index of refraction, l is the film thickness, and l_c is the coherence length of the quartz.[6,15] d_Q, independently measured as 1.13×10^{-9} esu,[6] is comparable to the values obtained for the corona-poled polymer films.[3,4] From eqs 2 and 3 it is observed that the angle of dopant orientation is related to $I_{film}^{1/2}$ and d_{film}. A relationship can be shown such that

$$(I_{film}/I_Q)^{1/2} \sim [a\langle\cos^3\theta\rangle + b\langle\cos\theta\sin^2\theta\rangle] \quad a,b = \text{constants} \quad (4)$$

Both terms contribute to the measured SHG intensity in this experiment. The important point is that the measured SHG intensity is related to the dopant orientation angle. More detailed descriptions of these relationships are available.[5,6,15]

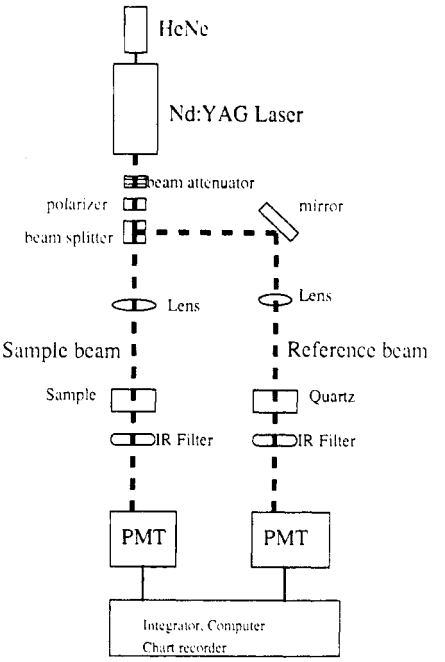

Figure 1. Schematic representation of the laser system used in the second harmonic generation experiment. Heavy dashed line represents beam path. HeNe = helium–neon laser (aligning beam); PMT = photomultiplier tube.

Figure 1 shows a schematic of the experimental apparatus. The laser light is generated by a q-switched Nd:YAG laser at 1.064 μm. The beam is p-polarized and split so that a y-cut quartz reference, used for monitoring laser power, and the sample are measured simultaneously. A photomultiplier and integrator collect and analyze the emergent SHG light (at 532 nm), and the optical signal is ratioed against the quartz reference.

Poling Techniques

Electric field induced corona and contact poling are used to orient the NLO dopants.[3-7,16] Poling involves applying a large electric field across the film normal to the surface, as shown schematically in Figure 2, so that the dopants align in the field direction. Poling can be performed at room temperature or at temperatures up to and above T_g, as long as the polymer has enough mobility and/or local free volume to allow the dopants freedom to rotate along the electric field vector. Dopants in a local microenvironment with sufficient mobility are free to rotate out of their imposed orientation and thus no longer contribute to the SHG intensity following poling. In situ (in the beam path) studies allow measurement of the SHG intensity increase during poling (rotation of the dopant into alignment due to the applied field), and the decay of SHG intensity after the field is removed can be examined without moving the sample and introducing error.

Corona poling[3c,4,6,7c,17,18] creates an electric field by generating a discharge from a metallic point source and placing a ground behind the film mounted across an air gap. The intense field generated at the needle tip creates gas ions with the same polarity as the needle that are accelerated toward and deposited on the film surface, creating a uniform, high-magnitude field across the material capable of efficiently orienting the NLO dopants.[4,7c] Corona onset and stability are a function of atmospheric conditions and electrode geometry.[4,17]

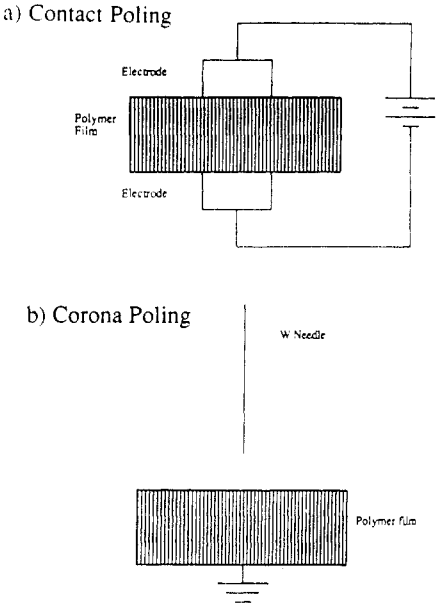

Figure 2. Schematic representation of the poling apparatus: (a) contact poling; (b) corona poling.

The electric field gradient created by the corona discharge is due to the ions deposited on the surface and to a smaller extent the carriers inherent in the material (space charges).[19] This gradient creates a net polarization across the film that generates a torque capable of rotating the dopants into orientation. The magnitude of the charge density is a function of the strength and polarity of the applied field, time relative to the field application, and temperature.[17-19] Corona poling is an attractive alternative to contact poling because it generates higher fields without causing sample breakdown and thus can orient a large number of dopants in a shorter time period and at lower temperatures than the other technique.[4,7c] However, the polymer mobility and free volume behavior and the effect of surface charge decay must be considered simultaneously when the overall temporal stability of corona-poled materials is examined.

Experimental Section

4-(Dimethylamino)-4'-nitrostilbene (DANS) (Kodak) was used as received and has been previously characterized.[3,4] PMMA (M_n = 46 400, M_w = 93 900) and PS (M_n = 117 000, M_w = 430 000) were obtained from Scientific Polymer Products. Polymer + 4 wt % DANS was dissolved in spectroscopic grade chloroform (PMMA) or in 1,2-dichloroethane (PS) to 10–20 g/L, mixed well, and filtered through a 10-μm glass frit filter. The solutions were then spin-coated onto soda lime glass. Spun films, 1.0–2.5 μm thick, were dried at ambient conditions for 24–48 h and then under vacuum for 24 h at 25 °C followed by elevated temperature (110 °C) for 24 h. Films were allowed to cool slowly under vacuum and stored in a drying oven at 70 °C prior to use. T_g's for the doped materials were measured via DSC (Perkin-Elmer DSC-2, 10 °C/min heating rate) as ca. 85 °C for PMMA and 88 °C for PS. Immediately prior to testing, the thermal history of all samples was erased by heating the film to 110 °C for at least 3 h. Samples were then cooled to the starting temperature (60, 95, or 110 °C) for the experiment, placed in the beam path, and allowed to equilibrate at that temperature for 1 h prior to applying the field.

The films investigated in this study involve polymers doped with 4 wt % optical dyes. This dopant concentration, lower than that commonly used in other[6,7,16] NLO studies, was initially chosen to obtain a high signal-to-noise ratio for the optical data when orienting the dopants via contact poling. Although the dopant concentration is too high to allow this to be a probe study of homopolymer behavior, this system is similar to or can be related to practical plasticized materials and composites. The possibility of dopant aggregation was considered by examining UV-visible and fluorescence spectra of DANS in solution and doped in films as a function of concentration. Upon examining the absorbance of DANS in dichloromethane between 350 and 550 nm over a concentration range covering 3 orders of magnitude up to 0.125 g/L, we found that the wavelength at which the maximum absorbance occurred did not change (436 ± 2 nm). Similar behavior was observed in the fluorescence spectra. The absorbance (maximum intensity at 416 ± 2 nm) and fluorescence (maximum intensity at 564 ± 2 nm) spectra show similar effects in PMMA films doped with dye concentrations ranging up to 5 wt %. No significant aggregation is observed. Dopant aggregation would decrease the net SHG intensity by allowing the dopants to align with their dipoles in a head-to-tail configuration (energetically more favorable) and decrease the net noncentrosymmetry.

The corona discharge was generated by a tungsten needle biased with −3000 V across a 0.6-cm air gap (relative humidity ~45% at 25 °C) normal to the polymer film. The corona current was limited to <8 μA. The SHG intensity characteristics are a function of poling parameters, including corona polarity, current, gap distance, humidity, and ambient environment.[4,17] Films quenched to final temperatures of 40 °C or above were cooled in 3–5 min, whereas films quenched to 25 °C cooled over a 7–10-min period. The field was applied in situ for 18 min in films quenched to 25 °C and for 15 min in all the other films. The reported SHG intensity is normalized to the sample thickness to allow comparisons to be made between a variety of films. Error limits due to noise in the SHG intensity measurements are less than or equal to twice the size of the symbols in Figures 3–5, with greater error at higher temperatures.

Surface voltage decay was measured with a Trek Model 341 high-voltage electrostatic voltmeter (ESVM). The ESVM drives the potential of a probe body to the same potential as the film surface voltage. This device measures the voltage independent of distance within 5 mm of the film surface without causing current flow, which would modify the data. After poling, the corona needle was removed, and the probe of the ESVM was placed 3 mm from the film surface. Surface voltage was measured as a function of time, with data taken every 5 s and averaged.

Results and Discussion

In situ SHG was used to examine dopant rotation in corona-poled films at temperatures between 25 and 110 °C, well below and above the measured T_g's of the doped polymer systems. Since the observed SHG intensity is related to the angle of dopant orientation and d_{film}, dopant orientation may be examined as a function of the local polymer microenvironment with time. The average of the absolute dopant orientation (obtainable by manipulating the beam polarization) is not considered here. The data discussed in the following sections examine relaxation behavior as a function of temperature with time and indicate that polymer relaxations cannot be solely responsible for the experimentally measured decay. This implies that decay due to surface charges created in the polymer during corona poling must be considered.

Effect of Thermal State above and below T_g. Investigation of Segmental Mobility on Dopant Orientation. The effect of thermal conditions on the local microenvironment surrounding the NLO dopants can be examined by using the in situ SHG approach. Films are heated to a poling temperature below or above T_g, corona poled, and quenched to or maintained at a final test temperature with the field maintained. The field is then removed, and the SHG intensity decay is measured with time at the given temperature.

Figure 3 presents $d_{film}/d_{film,max}$ as a function of time for PMMA + 4 wt % DANS films heated to 60 °C for 1 h, poled for 15 min at 60 °C, and either maintained at 60 °C or quenched to 40 or 25 °C. Each sample is tested with the polymer entirely in the glassy state. The increase in

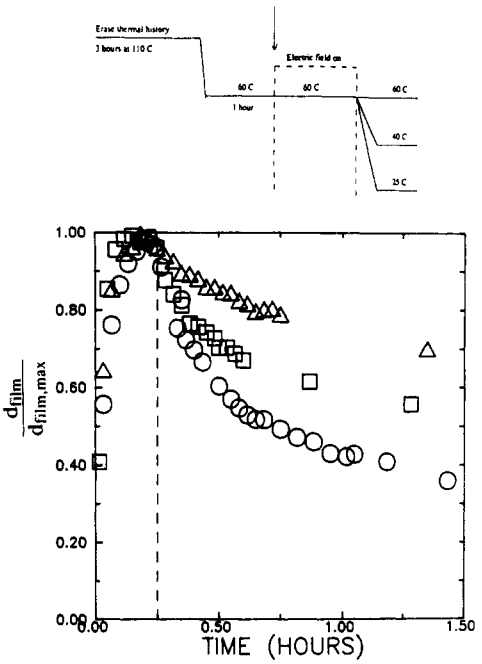

Figure 3. PMMA + 4 wt % DANS (4-(dimethylamino)-4′-nitrostilbene): Effect of temperature on the temporal stability of d_{film}. d_{film}, the second harmonic coefficient, is related to the angle between the applied electric field and an appropriate dopant molecular axis and is proportional to $I_{film}^{1/2}$, where I_{film} is the SHG intensity of the doped polymer film. The initial temperature is 60 °C, and the final temperatures after the field is removed are 60 (○), 40 (□), and 25 °C (△). Normalized values of $d_{film}/d_{film,max}$ versus time. Zero time denotes the time the electric field is applied, and the dashed line indicates the time the electric field is removed.

SHG intensity after the field is applied at zero time is due to the NLO dopants aligning noncentrosymmetrically in the field direction. A maximum in intensity is reached after 7–10 min of poling at 60 °C. The signal then decays about 5% during poling (due to charge effects, as discussed in the next section). Once the electric field is turned off, dopants in regions of sufficient mobility or sufficiently large local free volume have greater freedom to rotate out of their poling-imposed alignment. This dopant rotation results in a decay in the SHG signal intensity. At the same time, a persistent surface charge (resulting from the ions deposited on the film surface during corona poling) slowly decaying after the applied voltage is removed would maintain an electric field across the film, slowing down the dopant reorientation and tending to increase the temporal stability of the observed SHG intensity. The intensity decay is thus a combined measure of the surface charge decay and the loss of dopant orientation due to mobility/local free volume of the polymer matrix.

An attempt was made to fit the decays of d_{film} to the Williams–Watts (WW) stretchedexponential[20]

$$y = A \exp(-t/\tau)^{\beta} \qquad (5a)$$

where y represents $d_{film}(t)/d_{film}(t=0)$ (related to $[I_{film}(t)/I_{film}(t=0)]^{1/2}$), A is a constant, t is time with $t = 0$ being the time the applied field is removed, and τ is a characteristic relaxation time. β is a constant between 0 and 1 defining the nonideality of the exponential decay. A simplex-based nonlinear regression technique is used to fit experimental data.[5] In all cases the WW fit is not adequate to describe the measured relaxation behavior or did not give a unique solution. In particular, behavior of films quenched to temperatures well below T_g could not be properly fit due to the small amount of decay of the SHG intensity.

To simplify the fitting procedure, an approximation is made to fit the decay following the removal of the field as a biexponential of the form

$$y = \theta_1 \exp(-t/\tau_1) + \theta_2 \exp(-t/\tau_2) \qquad (5b)$$

with short-time relaxations characterized by τ_1 and long-time relaxations by τ_2. When fitting normalized data, the sum of θ_1 and θ_2 should equal 1. All best fit decay curves shown in the figures are generated with eq 5b. By using this approximation, we are not assuming that there are only two characteristic relaxation times but instead are recognizing that "fast" and "slow" characteristic times may approximate the multiplicity of relaxation times. Since τ_2 relates to the long-time relaxations, it may be related to the mobility in the polymer matrix. The effect of the surface charge decay is also contained in the calculated parameters for the fit. Equations of the form of eq 5b may not fit the data at time frames equivalent to τ_2 but are acceptable over the experimental times used in these experiments.

As the final temperature of the system decreases, the temporal stability of $d_{film}(t)/d_{film}(t = 0)$ increases. Equation 5b fails to describe exactly the short-time (<5 min) data, often giving initial magnitudes below 1 (ranging from 0.96 to 1.01) and predicting a more shallow intensity decay. The values for τ_1 and τ_2 for the samples poled at 60 °C and maintained at 60 °C ($\tau_1 \approx 0.3$ h, $\tau_2 \approx 5$ h) or quenched to 40 °C ($\tau_1 \approx 0.2$ h, $\tau_2 \approx 5$ h) are similar and are about half that for the samples quenched to 25 °C ($\tau_1 \approx 0.5$ h, $\tau_2 \approx 9$ h). Values for θ_1 increased with increasing final temperature (from 0.2 at 25 °C to 0.5 at 60 °C). As the sample is quenched to lower temperature, the segmental mobility surrounding the dopant is decreased, and the temporal stability of the dopant orientation is thus increased. A PS + 4% DANS film poled at 60 °C and quenched to 25 °C showed greater temporal stability of dopant orientation after the applied field is removed than a PMMA + 4% DANS film poled under the same conditions due to decreased segmental mobility in the PS matrix.[3d]

Data in Figure 4a represent $d_{film}/d_{film,max}$ data for PMMA + 4% DANS films poled at 95 °C (rubbery state). The films are maintained at 95 °C for 1 h following erasure of thermal history and then poled in situ at 95 °C for 15 min. They are then either maintained in the rubbery state at 95 °C or quenched to the glassy state at 60, 40, or 25 °C. All of the films reach a maximum in signal within 2–5 min after the field was turned on and then decay to a value of ca. 85% of the maximum value by the time the field is removed after 15 min. The maximum value of d_{film}/d_Q in films poled at 95 °C is ca. one-third greater than for the films poled at 60 °C. The rate of poling is rapid due to the large amount of local free volume and high segmental mobility in the polymer matrix above T_g. The decrease in $d_{film}/d_{film,max}$ during poling is more extensive in films poled at higher temperatures, indicating that the real charge and its distribution are also functions of poling temperature.

The rate of decay after the field is removed is a function of final film temperature. The decay of $d_{film}(t)/d_{film}(t=0)$ is shown in Figure 4b. Improved temporal stability is seen in films quenched to lower final temperatures. As the final temperature decreases from 95 to 40 °C, the values for both τ_1 and τ_2 increase. $\tau_1 \approx 0.1$ and $\tau_2 \approx 2$ h for the film poled and maintained at 95 °C, whereas $\tau_1 \approx 0.6$ and $\tau_2 \approx 20$ h for the film poled at 95 °C and quenched to 25 °C. As τ_2 and θ_2 increase with decreasing temperature (θ_2 is 0.19 at 95 °C and 0.87 at 25 °C), this implies that slow

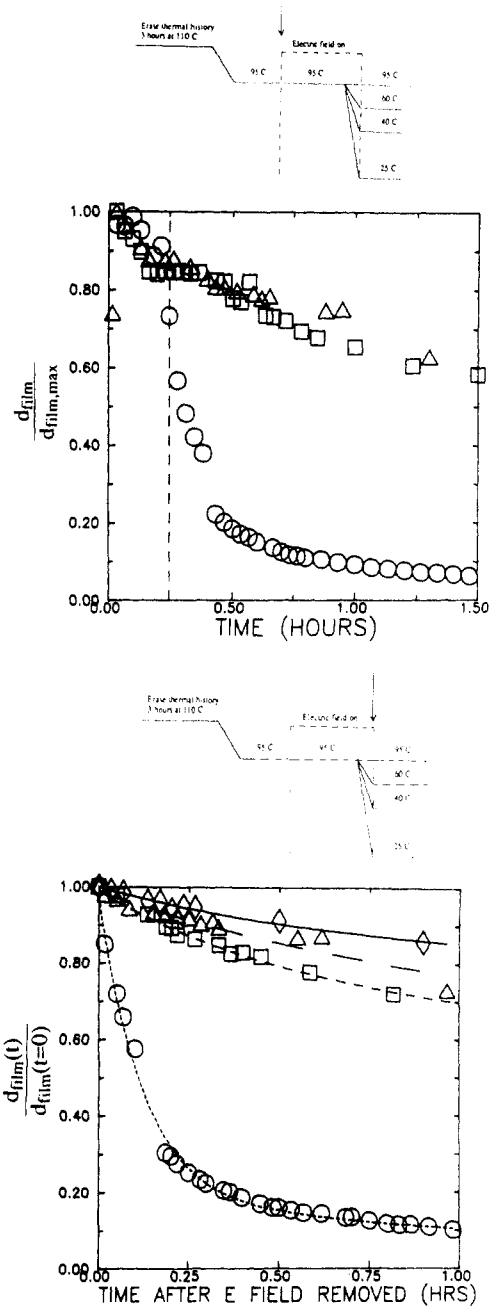

Figure 4. PMMA + 4 wt % DANS: Effect of temperature on the temporal stability of d_{film}. The initial temperature is 95 °C, and the final temperatures after the field is removed are 95 (○), 60 (□), and 40 °C (△). (Top (a)) Normalized values of $d_{film}/d_{film,max}$ versus time. Zero time denotes the time the electric field is applied, and the dashed line indicates the time the electric field is removed. (Bottom (b)) Normalized values of $d_{film}(t)/d_{film}(t=0)$ versus time after the field is removed. Final temperatures are 95 (○), 60 (□), 40 (△), and 25 °C (◇).

relaxation processes are more significant at lower temperatures.

$d_{film}/d_{film,max}$ was studied for PMMA + 4% DANS films heated to 110 °C while in the beam path and maintained at 110 °C for 1 h. The corona is then applied for 15 min, with the temperature maintained at 110 °C in the rubbery state, quenched to 95 °C (closer to T_g), or quenched into the glassy state at 60 or 25 °C. The field is then removed and the system maintained at the final temperature. Films poled at 110 and 95 °C show similar behavior during poling, with the signal maxima occurring within the first 1–3 min followed by a rapid decay. The rapid increase in $d_{film}/d_{film,max}$ at temperatures above T_g is due to the large degree

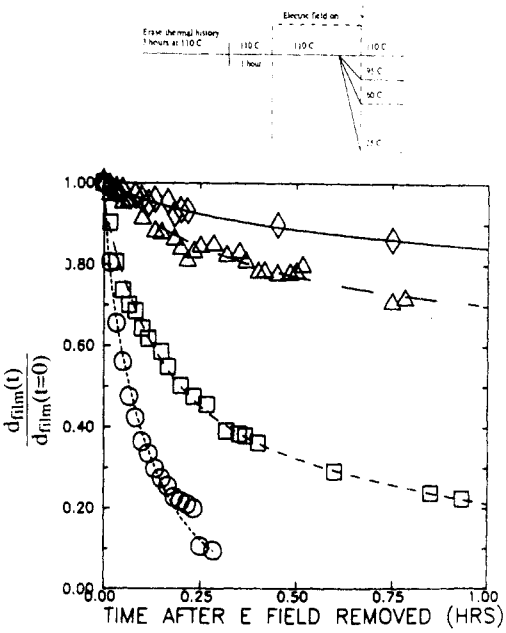

Figure 5. PMMA + 4 wt % DANS: Effect of temperature on the temporal stability of d_{film}. Normalized values of $d_{film}/d_{film,max}$ versus time after the field is removed. The initial temperature is 110 °C, and the final temperatures after the field is removed are 110 (○), 95 (□), 60 (△), and 25 °C (◇). Zero time denotes the time the electric field is removed.

of mobility and local free volume in the glassy matrix allowing the dyes to rotate freely into the field direction. The maximum magnitude of d_{film}/d_Q is about the same in films poled at 95 and 110 °C. The signal drops during poling to ca. 75–85% of its maximum. As the final temperature increases, the drop in signal that occurs during poling increases; this is more evident in films poled at 110 °C than in those poled at 95 °C. This drop is due to two contributions involving effects of polymer matrix mobility and the temperature-dependent surface/space charge.

Once the electric field is removed, the temporal stability of the second harmonic coefficient of the film poled and maintained at 95 °C is improved over films poled and maintained at 110 °C, as illustrated in Figure 5. Signal magnitudes are lower in films quenched from 95 °C than those quenched from 110 °C. Even at the highest temperatures above T_g, the signal decay, related to dopant mobility, occurs over a fairly long time scale. The decay data for the sample poled and maintained at 110 °C, at all times in the rubbery state, could not be adequately fit by a single-exponential equation. Functionalized NLO polymers corona poled above T_g show SHG intensity decays that were unable to be fit with a single exponential.[16d] As the quench temperature decreases from 110 to 25 °C, the values for both τ_1 and τ_2 increase by 1–2 orders of magnitude since the segmental mobility decreases.

It is interesting to compare films poled at 60 °C with those poled above T_g. The rates of poling are slower and the magnitudes of the signal maxima are decreased in the films poled below T_g at 60 °C (the maximum d_{film}/d_Q magnitude for films poled at 60 °C is ≈0.4 and for films poled at 95 and 110 °C is ≈0.6), due to the restricted segmental mobility hindering dopant rotation. The rate of signal decay following the removal of the applied field is more rapid in samples poled at 60 °C and maintained at 60 °C or quenched to 40 or 25 °C than in films poled above T_g and quenched to 60, 40, or 25 °C. Since the temperature is never raised above T_g in films poled at 60 °C, the amount and distribution of the local free volume are derived from the erasure of thermal history before

poling. The film is actually aging below T_g during the 1 h prior to poling, so the amount of local free volume in the system is smaller and the dopant rotation is more restricted than in those systems poled in the rubbery state.[3c] In the systems poled above T_g dopants can rotate more freely due to the greater segmental mobility and local free volume. In the films quenched from above to below T_g during poling, the local free volume and segmental mobility significantly decrease around the oriented dopant. This major change in local microenvironment should cause a greater restriction on the dopant mobility and have a greater effect on the temporal stability of the orientation over the time scale of these experiments. This implies that the local microenvironment surrounding the dopants in films poled at 60 °C undergoes a smaller degree of change during and following poling, which also explains the more rapid dopant disorientation.

Results similar to the above-T_g poling of PMMA + DANS films have been observed[3d] in a PS + 4% DANS system poled at 110 °C for 15 min and maintained at 110 °C or quenched to 95 or 60 °C. d_{film} reaches maximum values within 1–2 min and then decays with the field still applied, and decays more rapidly during poling in PMMA films than in PS films poled under the same temperature treatments. Smaller magnitudes and greater temporal stabilities following poling are observed in PS films when compared to PMMA films treated at the same temperatures. The maximum magnitude of d_{film}/d_Q is 3 times greater in PMMA than in PS films poled at 110 °C. This is consistent with results obtained for the temporal stability of SHG intensity of doped PS and PMMA films prepared via high-temperature (100 °C) contact poling.[3] As PS is a more rigid matrix than PMMA, the dopants have less freedom to rotate. PS systems reportedly have more restricted mobility or less sufficiently large regions of local free volume at a given temperature.[3d,5,11] It must be noted that PMMA is more polar than PS and may interact differently with the applied electric field,[3d,4] which may affect the observed temporal stability of d_{film}. In addition, there may be a small contribution to the observed differences in d_{film} from a solvatochromic effect of the matrix on the dopant.[3d]

The data discussed above indicate that thermal behavior cannot solely be responsible for the observed decay in SHG intensity seen during and following poling. The induced field gradient and the stability of the surface and space charges may contribute to the extent and rate of poling. The persistence of the space charge may influence the temporal stability of the dopant rotation following poling. It will be necessary to understand this effect to characterize the material behavior.

Effect of Corona-Induced Space Charge Field: Corona vs Contact Poling. Contact poling[3,5–7,16a–c,18] has been used to orient NLO dyes such as disperse red 1, 2-methyl-4-nitroaniline, and DANS doped in PMMA,[3,6a] PS, and polycarbonate[3] and functionalized on PS[16a,b] and PMMA.[6c] Earlier SHG studies on doped films either did not examine temporal stability[6a] or only examined the intensity decay after poling was complete.[3] To achieve reasonable levels of signal, high poling temperatures (rubbery state) were used with poling times up to 1 h.

Recent in situ SHG studies have been performed utilizing both contact[16a–c] and corona[16d] poling of functionalized NLO polymers. Gerbi et al.[16c] examined the decrease in SHG intensity with time following contact poling for PMMA films doped with 3-chloro-4-nitroaniline. For a film poled at 110 °C and quenched to room temperature with the field still applied, the SHG intensity dropped 50% within the first 30 s after the applied field was removed. Sixty-five hours later, the intensity dropped by only another 10%. Similar results are reported by Eich et al.,[16d] who examined the SHG intensity behavior of a polyethylene functionalized with a small dopant corona poled for 25 min above T_g (148 °C, no details of corona conditions given). No intensity maximum was observed during poling, and the intensity dropped by a factor of 5 immediately following the field removal and decayed to zero within the following 15–20 min. Eich's polymer[16d] is different from the majority of NLO materials studied for device applications (the dopant used in our study is about twice as large as the one used by Eich and should thus have improved rotational stability in a given matrix[3]) and should have a great deal of mobility above T_g so a rapid decay in intensity would be expected. This behavior is different from that observed in doped PMMA and PS films corona poled above T_g. This may be attributed to the different magnitudes and decay rates of the surface charges created within the various types of materials by the different poling techniques.[4,18]

Charge penetration also affects the surface charge. Corona discharge induced charge penetration, which may occur at higher temperatures,[19] is characterized by electrons or holes trapped at surface or near-surface sites. Trapped charges lead to a space charge layer at the film surface. In PMMA, due to the electronegativity of the ester side chain, electron mobility will be less than hole mobility. The buildup of trapped negative charge in surface sites will initially decrease the surface charge density and net electric field gradient by creating a more uniform charge density across the film, but will increase the lifetime of the field gradient and increase the temporal stability of the dopant orientation. As the temperature increases, the number of charge carriers increases ($\sim\exp(-A/T)$), increasing charge penetration effects. Differences in the SHG intensity with time in (+) and (−) polarity poled films have been studied in PMMA,[4] with (−) polarity poled films showing greater postpoling temporal stability.

The increase of d_{film} in the initial stages of corona poling is due to creation of the net electric field gradient across the sample. In films poled in air the ions deposited on the film surface may interact with surrounding water molecules and neutralize the surface charge. Studies have shown that the magnitude and temporal stability of the SHG intensity are related to the ambient atmosphere and humidity.[4] In addition, preliminary studies performed with similar polymers and poling conditions in dry neutral gas ambients indicate that surface voltage magnitudes and decay rates following poling are a function of ambient atmosphere and corona polarity.[4c] At higher temperatures, a greater value of d_{film} is observed. The more rapid rate of increase in d_{film} when the field is applied at time zero at temperatures above T_g is due to increased chain mobility and dopant rotational freedom. As the surface charge decays or is injected into the material, the magnitude of the field gradient decreases, causing d_{film} to decrease, consistent with the observed decrease during poling. The experimental observation that this decrease during poling occurs to a greater extent at high temperatures is consistent with the predicted temperature dependence of the surface voltage decay. Also, since increasing charge penetration occurs at higher temperatures, the decay during poling that occurs, particularly at 110 °C, could be due to a decrease in the effective path over which the gradient acts. A drop in d_{film} cannot be solely due to changes in the experimental temperature, since the drop also occurs in samples held at constant temperature during poling.

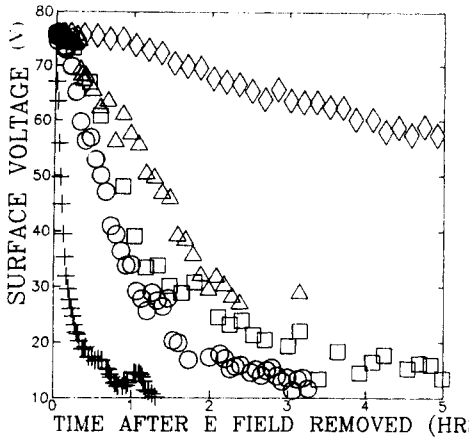

Figure 6. Surface voltage decay as a function of time for corona-poled PMMA + 4 wt % DANS films. Films were poled for 15 min at −3000 V for samples mounted on soda lime glass (SLG) and at −2500 V for the sample mounted on ITO. Films mounted on SLG were poled and maintained at 110 (○), 95 (□), 60 (△), and 25 °C (◇), and the film mounted on ITO was poled and maintained at 110 °C (+).

In contact-poled films, there is no decay during poling over the experimental time scales used in corona-poled films. More significantly, the near-instantaneous drop in intensity observed in contact-poled films following removal of the applied field[16a-c] is not seen in the corona-poled films studied here. These differences are due to the different characteristics of the two types of applied fields. This will be most significant at short times following removal of the applied discharge when the internal field is expected to be strongest. The important question arising from these considerations concerns the magnitude of the surface charge and the persistence of charge on the surface and in the bulk material. Since the magnitude of the electric field gradient across the film is related to the dopant orientation, this has significant implications on the dopant orientation and related SHG intensity.

The effect of surface voltage (SV) decay is examined in Figure 6. PMMA + 4% DANS films were heated to temperatures of 110, 95, 60, or 25 °C for 1 h, poled for 15 min, and maintained at the poling temperature after the field was removed. Following poling, the probe of the ESVM was placed 3 mm from the film surface, and the SV was measured with time. The initial magnitude of the SV is very small, only ≈75 V, particularly as compared to the applied voltage. (SV during corona poling is not measured.) SV remains constant in all samples for 3–8 min after poling and then begins to decay. As the poling temperature increases, SV decreases more rapidly. In all cases, the SHG intensity decays more rapidly than the corresponding SV.

At higher poling temperatures, the shapes of the SHG and SV decay curves are more similar. For example, the SHG intensity of films poled and maintained at 110 °C decays to ca. 35% of its initial intensity in 0.13 h; after 1.5 h the SV decays to 35% of its initial value. The sample poled and maintained at 60 °C retained ca. 40% of its initial SHG intensity 1.5 h after the field was removed; after 1.5 h, the SV is still at 60% of its initial magnitude. Temperature affects the surface and space charges due to the combined effects of the temperature dependence of the corona discharge current (slight) and charge penetration.[4,5,17]

The initial magnitude of the SV is ca. 75 V across the ≈2-μm-thick PMMA film + 1.2-mm-thick soda lime glass, giving a field across the film surface to ground of ca. 625 V/cm, significantly less than the ≈0.5 MV/cm fields commonly used to contact pole doped polymer films.[3,5,6] The significance of this result is that field strengths 3 orders of magnitude less than that usually employed to contact pole NLO dopants can affect the SHG decay rate. This is seen by comparing the sharp drop off in SHG intensity that occurs immediately after the applied field is shut off in contact poling with the continuous but much slower intensity decay observed in corona-poled systems immediately after the discharge is removed. In the thinner PS films (≈1.5 μm), higher initial SV magnitudes (≈200 V) are observed. The SV decays rapidly to ca. 150 V in the first 10 min but retains a value of ≈100 V 6 h after the poling field is removed. This different behavior relates to differences in the charge mobility in PS and PMMA, with the charge having greater difficulty penetrating into and moving through the PS film. The initial voltage drop is possibly due to recombination/reaction of the ions on the film surface with ambient molecules.[5,18]

Preliminary results indicate that in PMMA films doped with 4 wt % DANS and poled at 25 °C in air, the SV does not completely dissipate until more than 15 h following poling. Due to the polar dyes, the SV decays much more rapidly in doped than in undoped PMMA, with the latter losing only ca. 20% of its initial SV in the first 100 h after poling at 25 °C for 15 min. Dopant concentration thus affects the temporal stability of the SV. This will affect the temporal stability of dopant orientation and thus the SHG intensity and should be considered when comparing stability data for a variety of samples.[4,5]

In the samples examined in these experiments, the thickness of the space charge region includes the polymer film + soda lime glass (SLG). The dielectric constant of the glass is about twice that of the polymer. When comparing the charge behavior of the two-layer sample to that of just the polymer film, one should observe different temporal behavior. This was tested by spinning films of the same doped polymers as spun onto SLG onto the conductive coated side of indium tin oxide (ITO) glass and measuring the SV decay after similar poling treatments. The conductive coating of the ITO can be grounded, so that the effective space charge region only includes the polymer film. The SV decay of a film mounted on ITO and poled and maintained at 110 °C is shown in Figure 6. The poling voltage was limited to −2500 V to maintain a corona current identical with that of the SLG-mounted samples. Again the initial measured SV is independent of temperature. However, the net field across the film mounted on ITO is ≈75 V/2 μm ≈ 0.38 MV/cm as opposed to ≈625 V/cm. The initial SHG intensity is significantly greater in the ITO films.[4c] Since the charge only needs to travel a short distance before it reaches ground, the resistance is reduced. The temporal stability of the surface charge is significantly lower, particularly at higher temperatures where charge penetration is favored. Films spun onto ITO were also poled at 60 and 25 °C, and it was observed that the more rapid decay of the SV seen on the films mounted on ITO was significant mainly over short time scales (<≈1.5 h at 110 and 60 °C), after which the voltages approach the same values as for the films poled on SLG. Samples poled on ITO showed increasing temporal stability with decreasing poling temperature similar to those films poled on SLG.

With the present experimental setup, approximately the first 15 s of the SV decay following the field removal is not measured. During this time frame it can be assumed that a large drop in SV occurs, since the SV during corona poling should be significantly higher (due to the very large applied corona voltage). Improved experimental apparatus

will allow for more rapid measurements to be made, and results will be reported.[4c] However, since no significant, rapid decrease in the SHG intensity is observed immediately upon removal of the applied field, the SHG decay rate must be significantly affected by the persistence of the SV.

Summary

The effect of temperature above and below T_g on the rotation of NLO dopants in corona-poled amorphous polymer matrices can be examined by using in situ SHG. The polymer relaxation behavior and corona-induced electric field, both dependent on temperature and time, influence the magnitude and temporal stability of the dopant orientation following removal of the applied field. When the field is applied, the SHG intensity and d_{film}/d_Q increase as dopants in regions of sufficient mobility and local free volume align in the field direction. At poling temperatures above T_g, the SHG intensity and d_{film}/d_Q increase, reach a maximum, and then decay with the field still applied. At poling temperatures below T_g, the rate of signal increase is slower and the maximum intensity and the amount of decay during poling is lower. This decay during poling is due to surface/space charge effects induced in the film by the applied field. Once the applied field is removed, the SHG signal decays with time as a function of temperature, with increasing temperature creating greater segmental mobility and local free volume that allow more facile dopant rotation. Dopant disorientation is related to polymer relaxation phenomena and surface charge persistence. The surprisingly low surface voltage observed on these films following corona poling significantly affects the dopant rotation dynamics. The persistence of the SV increases the temporal stability of the dopant orientation particularly at short times. The nearly instantaneous, large-magnitude drop in SHG intensity seen in contact-poled films upon removal of the applied field is not observed in these corona-poled films due to the persistence of the surface charge. The SV is more temporally stable at lower temperatures. Since the time scale of the persistence of the SV is on the same order as the polymer relaxations at short times, both processes affect the SHG measurements over the time frame of these experiments.

Acknowledgment. We thank Dr. L. Michael Hayden (Unisys Corp.) for helpful discussions about corona poling and gratefully acknowledge the support of Unisys and the Materials Research Center at Northwestern University (Grant DMR88-20280); J.M.T. also acknowledges NSF through its Presidential Young Investigator Program, and H.L.H. acknowledges a fellowship from IBM. We appreciate helpful discussions with Dr. S. G. Grubb and Ms. S. J. Bethke of Amoco Technology Co. and Dr. Gary Boyd of 3M. We thank Trek, Inc. (Medina, NY), for lending us a Model 341 electrostatic voltmeter.

References and Notes

(1) (a) Department of Materials Science and Engineering. (b) Department of Physics and Astronomy. (c) Department of Chemical Engineering.
(2) This work was presented in part at the American Physical Society Meeting, St. Louis, March 1989.
(3) (a) Hampsch, H. L.; Yang, J.; Wong, G. K.; Torkelson, J. M. *Polym. Commun.* **1989**, *30*, 40. (b) Hampsch, H. L.; Yang, J.; Wong, G. K.; Torkelson, J. M. *Macromolecules* **1988**, *21*, 526. (c) Hampsch, H. L.; Yang, J.; Wong, G. K.; Torkelson, J. M. *Macromolecules*, following paper in this issue. (d) Hampsch, H. L.; Yang, J.; Wong, G. K.; Torkelson, J. M. In *New Materials for Nonlinear Optics*; Stucky, G., Marder, S., Sohn, J., Eds.; ACS Symposium Series, American Chemical Society: Washington, DC, in press.
(4) (a) Hampsch, H. L.; Wong, G. K.; Torkelson, J. M.; Bethke, S. J.; Grubb, S. G. *Proc. SPIE* **1989**, *1104*, 268. (b) Hampsch, H. L.; Torkelson, J. M.; Bethke, S. J.; Grubb, S. G. *J. Appl. Phys.* **1990**, *67*, 1037. (c) Bethke, S. J.; Grubb, S. G.; Hampsch, H. L.; Torkelson, J. M. *Proc. SPIE*, in press.
(5) Hampsch, H. L. Ph.D. Thesis, Northwestern University, 1990.
(6) Williams, D. J., Ed. *Nonlinear Optical Properties of Organic and Polymeric Materials*; ACS Symposium Series 233; American Chemical Society: Washington, DC, 1982. Chemla, D. S.; Zyss, J., Eds. *Nonlinear Optical Properties of Organic Molecules and Crystals*; Academic Press: New York, 1987; Vols. 1, 2.
(7) (a) Singer, K. D.; Sohn, J. E.; Lalama, S. J. *Appl. Phys. Lett.* **1986**, *49*, 248. (b) Singer, K. D.; Kuzyk, M. G.; Sohn, J. E. *J. Opt. Soc. Am. B* **1987**, *4*, 698. (c) Singer, K. D.; Kuzyk, M. G.; Holland, W. R.; Sohn, J. E.; Lalama, S. J.; Comizzoli, R. B.; Katz, H. E.; Schilling, M. L. *Appl. Phys. Lett.* **1988**, *53*, 1800.
(8) Boyd, G. *Thin Solid Films* **1987**, *152*, 295; *J. Opt. Soc. Am. B* **1989**, *6*, 685.
(9) Peterson, K. A.; Zimmit, M. B.; Fayer, M. D.; Jeng, Y. H.; Frank, C. W. *Macromolecules* **1989**, *22*, 874.
(10) Lee, A.; Wool, R. P. *Macromolecules* **1986**, *19*, 1063. Hobbs, J. P.; Sung, C. S. P.; Kirshnan, K.; Hill, S. *Macromolecules* **1983**, *16*, 193.
(11) Victor, J. G.; Torkelson, J. M. *Macromolecules* **1988**, *21*, 3490; **1987**, *20*, 2951, 2241. Royal, J. S.; Victor, J. G.; Torkelson, J. M. *Macromolecules*, submitted.
(12) Yu, W.-C.; Sung, C. S. P.; Robertson, R. E. *Macromolecules* **1988**, *21*, 355. Yu, W.-C.; Sung, C. S. P. *Macromolecules* **1988**, *21*, 365.
(13) Crisman, J. M.; McKenna, G. B. *J. Polym. Sci., Polym. Phys. Ed.* **1987**, *25*, 1667. Heijboer, J. In *Static and Dynamic Properties of the Polymeric Solid State*; Penthrick, R., Richards, R., Eds.; D. Reidel Publishing Co.: Amsterdam, 1982.
(14) Michel, P.; Dugas, J.; Carior, J. M.; Martin, L. *J. Macromol. Sci.—Phys.* **1986**, *25*, 379.
(15) (a) Shen, Y. R. *Principles of Nonlinear Optics*; Wiley: New York, 1984. (b) Bloembergen, N. *Nonlinear Optics*; W. A. Benjamin, Inc.: New York, 1965. (c) Singh, S. In *CRC Handbook of Laser Science and Technology*; Weber, M. J., Ed.; CRC Press, Inc.: Boca Raton, FL, 1986; Vol. III.
(16) (a) Ye, C.; Marks, T. J.; Yang, J.; Wong, G. K. *Macromolecules* **1987**, *20*, 2322. (b) Hubbard, M. A.; Minami, N.; Ye, C.; Marks, T. J.; Yang, J.; Wong, G. K. *Proc. SPIE* **1989**, *971*, 110. (c) Gerbi, D.; Boyd, G. T.; Ender, D. A.; Henry, R. M.; Kam, K. K.; Leung, P. C. W.; Stofko, J. J. Presentation at the Topical Workshop on Organic and Polymeric Nonlinear Optical Materials, American Chemical Society, Division of Polymer Chemistry, May 1988. (d) Eich, M.; Sen, A.; Looser, H.; Bjorklund, G. C.; Swalen, J. D.; Tweig, R.; Yoon, D. Y. *J. Appl. Phys.* **1989**, *66*, 2559. (e) Eich, M.; Renk, B.; Yoon, D. Y.; Wilson, C. G.; Bjorklund, G. C. *J. Appl. Phys.* **1989**, *66*, 3241.
(17) Williams, E. M. *The Physics and Technology of Xerographic Processes*; Wiley-Interscience: New York, 1984. McDaniel, E. W.; Mason, E. A. *The Mobility and Diffusion of Ions in Gasses*; Wiley-Interscience: New York, 1978.
(18) (a) Sessler, G. M., Ed. *Electrets*; Springer-Verlag: Berlin, 1980. (b) Hill, R. M. *J. Phys. C* **1975**, *8*, 2488. (c) Li, J. R.; Wintle, H. J. *J. Appl. Phys.* **1989**, *65*, 4617. (d) Seanor, D. A. In *Polymer Science*; Jenkins, A. D., Ed.; North-Holland: Amsterdam, 1972.
(19) Carr, S. H. In *Electrical Properties of Polymers*; Seanor, D. A., Ed.; Academic Press: New York, 1982. van Turnhout, J. *Thermally Stimulated Discharge of Polymer Electrets*; Elsevier: Amsterdam, 1975.
(20) Williams, G.; Watts, D. C. *Trans. Faraday Soc.* **1970**, *66*, 80.